J Polym Environ (2009) 17:212–224
DOI 10.1007/s10924-009-0141-z

ORIGINAL PAPER

The Shape Memory Properties of Biodegradable Chitosan/Poly(L-lactide) Composites

Qinghao Meng · Jinlian Hu · KaiChiu Ho · Fenglong Ji · Shaojun Chen

Published online: 8 October 2009

Abstract The shape memory behavior of PLLA (poly (L-lactide)) and chitosan/PLLA composites was studied. PLLA and chitosan were compounded to fabricate novel materials which may have biodegradability and biocompatibility. Chitosan does not significantly affect the glass and melting transition temperature of the PLLA. Both the pure PLLA and chitosan/PLLA composites showed shape memory effect arising from the viscoelastic properties of PLLA comprised of semi crystalline structures. The shape recovery ratio of the chitosan/PLLA composites decreased significantly with increasing chitosan contents due to the incompatibility between PLLA and chitosan. Phase separation structures of the composites were observed by using atomic force microscopy. To obtain good shape memory effect, the chitosan content should be below 15 wt%.

Keywords Shape memory property · Poly(L-lactide) · Chitosan

Introduction

Shape memory polymers are a group of 'actively moving' polymers which have at least dual shape capability. A permanent shape can be given to them by a processing step or a heat setting process. The polymers can rapidly change their shapes in a predefined way from one to another under appropriate stimuli such as heat [1], electricity [2], pH value [3], ionic strength [4], light [5] and magnetic field [6]. Shape memory polymers can be used in smart textiles and apparels [7, 8], intelligent medical devices [9–14], heat shrinkable films for electronics packaging [15], and self-deployable sun sails in spacecrafts in the forms of solution, emulsion [16–18], film [19], fiber [8, 20–24], nanofiber [24–34], foam [35–38] or bulk [39].

The medical applications of shape memory polymers are of great interest to scientists and engineers due to their combination of biocompatibility with their wide range of tunable stiffness, tailorable transition temperatures, fast actuation, large deformation, large recovery, and elastic properties [40]. The medical applications of shape memory polymers presently reported include: laser or magnetic activated shape memory devices for the mechanical removal of blood clots [41–45]; aneurysm coils for the treatment of intracranial aneurysm in place of platinum coils [46]; biodegradable shape memory sutures for surgery [9, 47, 48]; shape memory foams for overweight patients to lose weight [37]; shape memory foams for drug delivery to treat disorders and diseases in the stomach or intestine [11, 49]; and shape memory polymer for orthodontic appliances [50–52]. The shape memory polymers with biodegradability would be beneficial for many applications because they do not require a second surgery to remove the materials if necessary because the polymer would gradually dissolve in the body due to the biodegradability of the materials.

PLLA is a biodegradable and biocompatible linear aliphatic biopolymer derived from 100% renewable resources such as corn and sugar beets. It can be readily degraded by hydrolysis under mild conditions to lactic acid, which is a common biodegradable organic acid naturally present even

Q. Meng · J. Hu (✉) · F. Ji · S. Chen
Institute of Textiles and Clothing, The Hong Kong Polytechnic University, Hung Hom, Kowloon, Hong Kong, People's Republic of China
e-mail: tchujl@inet.polyu.edu.hk

K. Ho
The Hong Kong Research Institute of Textiles and Apparel, Kowloon, Hong Kong, People's Republic of China

in the human body [53, 54]. PLLA has been widely used in biomedical applications, such as surgical sutures and implants [55], drug delivery systems [56, 57], three-dimensional porous scaffolds for tissue engineering applications [58, 59] and bone fixation [60, 61].

The shape memory effect of PLLA has been studied by several researchers [62–67]. It was found that the shape recovery of PLLA decreased and approached to steady with thermomechanical cyclic tensile testing number increasing. Zheng et al. [68] investigated the shape memory effect of poly(D,L-lactide)/hydroxyapatite composites which are also for potential biomedical applications. They assumed that the amorphous poly(D,L-lactide) polymer forms a reversible phase and the crystalline calcium phosphate forms a stationary phase, which were necessary for the composites to show good shape memory effect. They found that the hydroxyapatite particles improved the shape memory effect of poly(D,L-lactide).

Chitosan (poly(*N*-acetyl-D-glucosamine-co-D-glucosamine)) is a partially *N*-deacetylated derivative of chitin(poly(*N*-acetyl-D-glucosamine)), which is the second most abundant biopolymer in nature after cellulose. Chitosan is biocompatible, nontoxic, edible, and biodegradable. In addition, chitosan has antimicrobial activities against different groups of microorganisms [69–72]. It has been widely used for medicine, edible packaging or coating, food additives, cosmetic, water treatment and antifungal agents.

Many efforts have been made to compound polylactide and chitosan through chemical methods or physical methods to prepare materials with novel functions. Zhu et al. [73] covalently immobilized chitosan onto polylactide films using a photosensitive hetero-bifunctional crosslinking reagent, 4-azidobenzoic acid by irradiating with ultraviolet light. Chitosan molecules immobilized on the polylactide could be modified by heparin (Hp) solution to form a polyelectrolyte complex on the polylactide surface. The polylactide surface modified by chitosan/heparin complex could inhibit platelet adhesion and activation. Li et al. [74] prepared a series of chitosan/polylactide composites as a scaffold material because pure polylactide has obvious weaknesses of fast biodegradation, acidic degradation product, hydrophobicity, and acidic degradation product. It was showed that the composites were hydrophilic and had appropriate porosity and structure, which were favorable to cell growth. The degradation tests in vitro indicated that the degradation speeds of the materials were slower than that of polylactide, and the materials could keep adjacently litmusless, certain shape and mechanical properties. Suyatma and Sébastien et al. [75, 76] prepared biodegradable film blends of chitosan/polylactide by solution mixing and film casting. The films were intended to be used for antimicrobial food bio-packaging with good water vapor barrier properties. They found the composite films had good water barrier properties and antifungal activity at suitable composites.

In this study, we prepared chitosan/PLLA composites by solution casting and studied the shape memory effect of the composites. The thermal properties, dynamic mechanical properties and phase separation of the composites were investigated to illustrate the influence of chitosan on the shape memory effect of PLLA. The biomaterial chitosan/PLLA with shape memory effect may be used for drug controlled release and biodegradable smart devices which can be implanted into bodies. In addition, the PLLA incorporated chitosan may have antibacterial properties, therefore the composites may be used for intelligent packaging with antibacterial effects.

Experimental

Material

Chitosan (Jinan Haidebei Marine Bioengineering Co., Ltd, China) was prepared from shrimp shells by acid and alkali treatments. The degree of deacetylation was about 85%. It was pulverized into powder, the size of which was below 150 um. The PLLA was synthesized by ring-opening polymerization of cyclic lactic monomers. Tin(II) 2-ethylhexanoate was used as catalyst. The viscosity average molecular weight of the PLLA was 49,000. The solvents for solution blending were acetic acid (Aldrich, USA) and chloroform (Aldrich, USA). The FT-IR spectrum of the PLLA is shown in Fig. 1. It is consistent with that reported in the literature [77]. The characteristic IR peak at around 1761 cm^{-1} is due to the C=O stretching vibration. The peaks at about

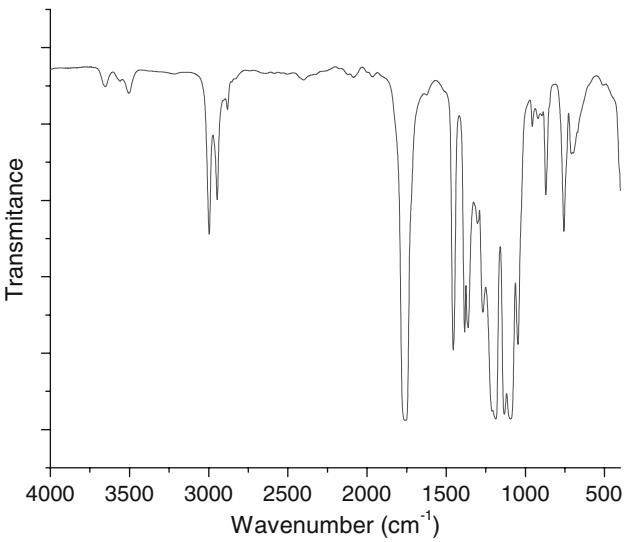

Fig. 1 FT-IR spectrum of the PLLA

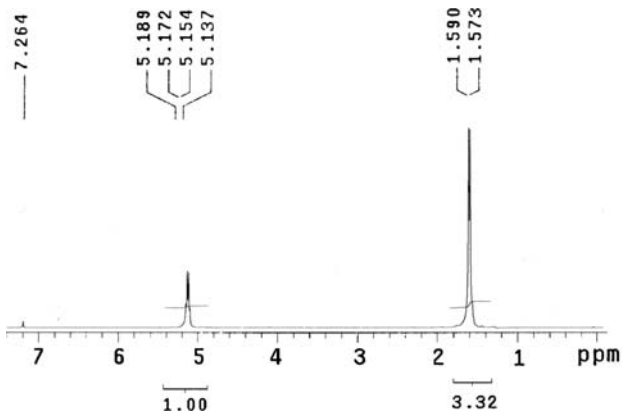

Fig. 2 NMR spectrum of the PLLA

1187 cm^{-1} and 1093 cm^{-1} are owing to the asymmetry stretching vibration and symmetry stretching vibration of C–O–C. The peaks at about 2997 cm^{-1} and 2946 cm^{-1} are attributed to the stretching vibration of $–CH_3$. The peak at 3506 cm^{-1} corresponds to –OH stretching vibration. The ^{1}H-NMR spectrum of the PLLA characterized with a Varian Unity INOVA Solid State (400 MHz) FT-NMR Spectrometer is shown in Fig. 2. $CDCl_3$ was used as the solvent and tetramethylsilane was used for the internal reference. The resonances at 1.573 and 1.590 ppm are ascribed to the protons of methyl groups in the PLLA. The resonances at 5.137, 5.154, 5.172 and 5.189 ppm are ascribed to the protons of methine groups in PLLA.

Sample Preparation

Chitosan and PLLA were first dissolved separately in acetic acid (1 wt%) and chloroform (1 wt%). After the chitosan and PLLA were completely dissolved, the two solutions were blended with vigorous mechanically stirring until a homogenous solution was prepared. Then films were made by casting the mixed solution into polytetrafluoroethylene coated plates. In order to make pinhole free films, the solution was first degassed at 50 Pa for 30 min. Then the solvent was evaporated at 60 °C for 12 h at atmospheric pressure and the residual solvent was removed at 60 °C for another 12 h in a vacuum oven. The thickness of the obtained films was about 0.10 mm. Wires of about 2 mm in diameter of the PLLA and the composites were prepared using a Haake minilab (Thermo Electron Corporation) at an extruding temperature of 160 °C.

Characterization

The thermal properties of the PLLA and its composites were determined using a DSC (Perkin–Elmer Diamond Differential Scanning Calorimeter) with nitrogen as purge gas. Indium and zinc were used for calibration. First, samples were heated to 200 °C at a heating rate of 10 °C/min and maintained at 200 °C for 3 min to remove thermal history, and subsequently cooled to 22 °C at a cooling rate of 25 °C/min. Finally, samples were reheated at a 10 °C/min heating rate to 200 °C. The heat flow change with temperature was recorded.

The DMA (Dynamic Mechanical Analysis) test was carried out on a Perkin–Elmer Diamond Dynamic Mechanical Analyzer operated in the tensile mode. Samples of 30 × 5 × 0.5 mm^3 in dimension were cut out from the cast films using a sharp knife for DMA testing. The heating rate was 2 °C/min, frequency 1 Hz, and oscillation amplitude 5.0 μm. Tests were conducted over the temperature range from 0 to 200 °C. The gauge length between the clamps was 15 mm.

The shape memory effect was first roughly examined by field observation. First, the extruded straight wire was folded 180° in 65 °C water. Second, the folded wire was taken out from the hot water and cooled to the ambitent temperature to retain the deformed shape. After 2 min, the folded wire was put into 65 °C water again to observe the shape recovery.

The shape fixity and recovery ratio of the PLLA and the PLLA composites were determined by thermomechanical cyclic tensile testing using tensile tester (Instron 5566) equiped with a self-fabricated temperature-controllable chamber. Samples of 40 × 5 × 0.5 mm^3 in dimension were cut out from cast films. The sample gauge length was 20 mm. The cyclic tensile testing path is shown in Fig. 3. ε_m is the defined maximum deformation in the cyclic tensile testing. ε_u is the strain after unloading at below the switch temperature, and $\varepsilon_p(N)$ is the residual strain after recovering in the Nth cycle. The thermomechanical cycle for measuring the shape

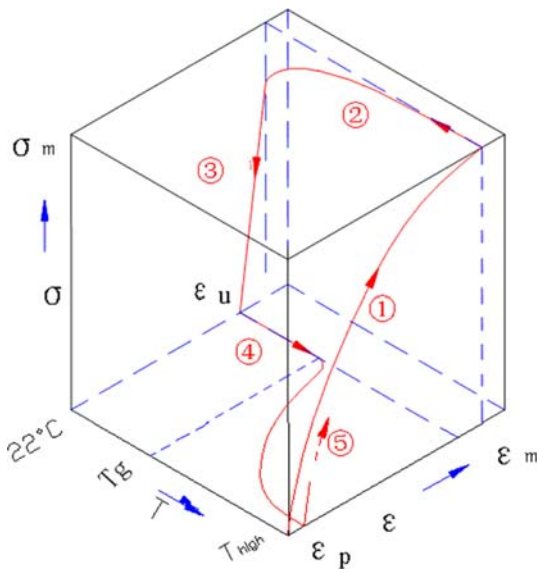

Fig. 3 Schematic thermomechanical cyclic tensile testing path

memory properties is as follows: (1) The film was first stretched to ε_m at 65 °C (T_{high}) at a drawing speed of 10 mm/min [78]; (2) Subsequently, cool air was vented passively into the chamber to cool down the sample to 22 °C and the deformation was maintained for 2 min to fix the temporary elongation; (3) Then upper clamp was returned to the original position at a speed of 40 mm/min and the film shrank from ε_m to ε_u because of instant elastic recovery; (4) Finally, the film was heated to 65 °C to allow shape memory recovery with result film elongation returning to ε_p; (5) After finishing the above procedures, the second cycle began. The ε_m was set as 50, 100 and 200% to investigate the influence of defined maximum deformation strain on the shape memory effect. The cycle was repeated for five times. The shape fixity ratio ($R_f(N)$) and shape recovery ratio $R_{r\cdot tot}(N)$ after Nth cycle are calculated according to the following equations [23, 79–81]:

$$R_f(N) = \varepsilon_u(N)/\varepsilon_m \times 100\,\%$$

$$R_{r\cdot tot}(N) = \left(\varepsilon_m - \varepsilon_p(N)\right)/\varepsilon_m \times 100\,\%$$

The micromorphology observation of the composites was conducted through a probe atomic force microscopy (AFM) (SPA-300HV, Seiko Instruments) in the tapping-mode. NANOSENSORS™ PPP-SEIHR AFM probes (Seiko Instruments/high force constant) were used. The silicon cantilever spring constants was 15 N/m, length 225 um and resonance frequency 130 kHz. Height and phase images were recorded simultaneously.

Results and Discussion

Thermal Properties

Figure 4 shows the DSC curves of PLLA and chitosan/PLLA composites at different chitosan contents. All the samples exhibit a two indistinctive glass transition feature at about 32 and 61 °C [82, 83]. As shown in Fig. 5, the glass transitions show as a prominent one in the cooling scan at a cooling rate of 25 °C/min. No significant T_g change is observed both on the heating scan and cooling scan of chitosan/PLLA composites at different chitosan contents.

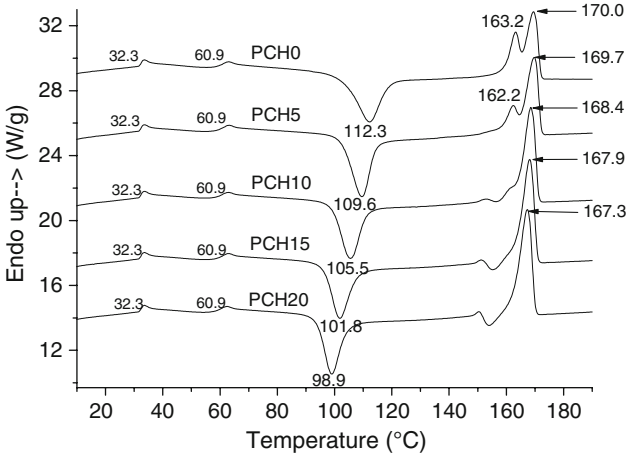

Fig. 4 DSC second heating curves of the composites at different chitosan contents

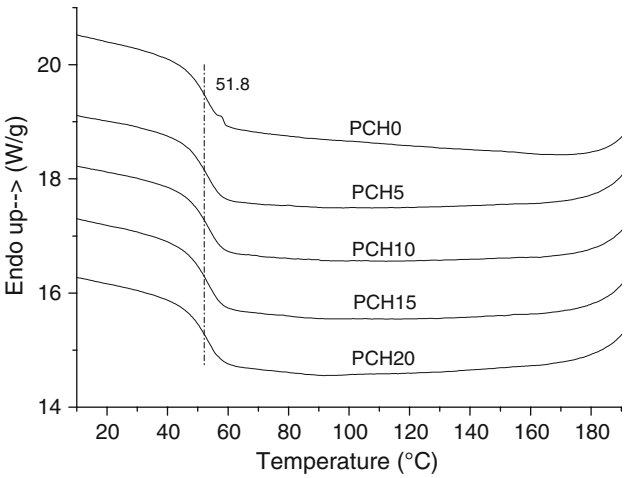

Fig. 5 DSC cooling curves of the composites at different chitosan contents

The thermal transition as shown in Fig. 4, at around 99–112 °C is attributed to the cold crystallization of PLLA. This crystallization exothermic peak appearing prior to the major melting endothermic peak in the heating scans is an additional crystallization. The cold crystallization transition temperature of the chitosan/PLLA decreases markedly with increasing chitosan contents. This may be because chitosan acts as a nucleating agent, promoting a faster crystallization of PLLA [84–87].

The thermal transition at the high temperature from 150 to 170 °C showing in Fig. 4 is due to the melting transition of PLLA [88]. The low-temperature melting endotherm of the double-peak transition may be attributed to the melting of the primary crystals formed during the first cooling, while the high temperature melting endotherm is owing to the melting of the re-crystallized crystals formed during the heating scan [89–91]. For the pure PLLA, the first melting transition temperature and the second melting transition temperature are 163 and 170 °C. With increasing chitosan content, both peak positions decrease slightly from the melting peak of the pure PLLA.

In conclusion, the DSC results suggest that the chitosan/PLLA composites have a two-phase structure: a crystalline phase which has a high temperature melting transition and a glassy state phase which has low temperature glass transitions. The chitosan has no significant influence on the glass transition of the PLLA. However, it decreases the

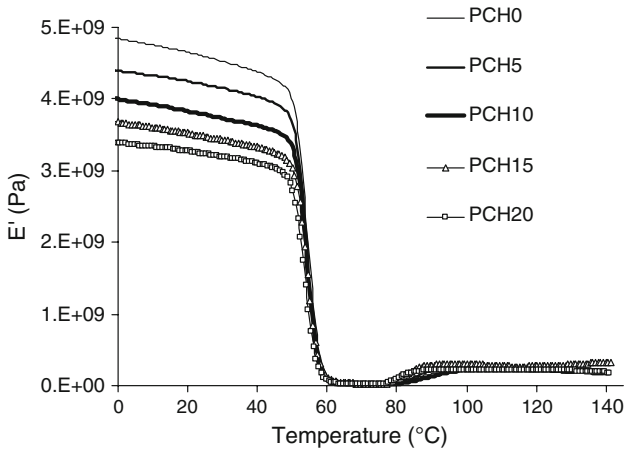

Fig. 6 Log E′—temperature curves of the chitosan/PLLA

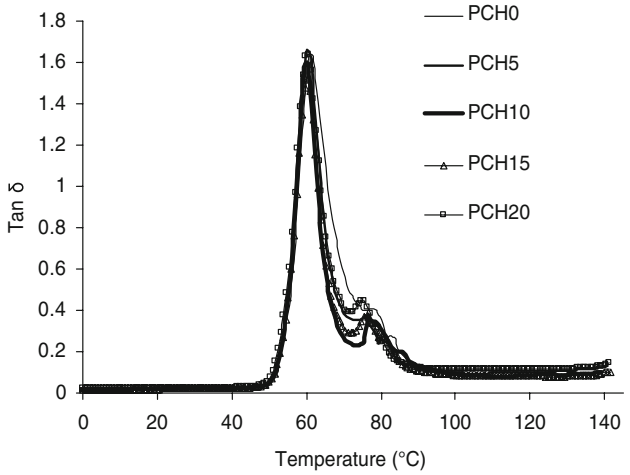

Fig. 7 Tan (δ)—temperature curves of the chitosan/PLLA

melting temperatures of the PLLA slightly with increasing chitosan contents.

Dynamic Mechanical Analyses

The elastic modulus (E′) and loss tangent (tan δ) of the PLLA with different chitosan contents are given in Figs. 6 and 7 respectively. The elastic modulus of all the samples displays a sharp decrease at about 60 °C and the loss tangent shows a peak at this temperature correspondingly, which indicates the glass transition of the PLLA. At a temperature of above 60 °C, all the samples show a plateau elastic modulus, suggesting a rubberlike structure of PLLA composed of both crystalline and amorphous phases. The slight increase of the elastic modulus at above 80 °C is attributed to the cold crystallization because, at this temperature, the PLLA chains obtain enough mobility to crystallize. This result is consistent with that obtained in the DSC section. The elastic modulus change trend of pure PLLA and chitosan/PLLA composites is very similar to that of a shape memory polyurethane consisting of hard and soft-segment phases [92]. The PLLA and its composites are like a shape memory rubber composing of both crystalline and amorphous phases. The large modulus decrease at the transition temperature is a prerequisite for the material to exhibit shape memory effect.

Figure 7 also indicates that the glass transition temperature of the chitosan/PLLA composites is not significantly affected by chitosan. However, the elastic modulus of chitosan/PLLA decreases markedly with increasing chitosan contents at the temperature below the glass transition temperature.

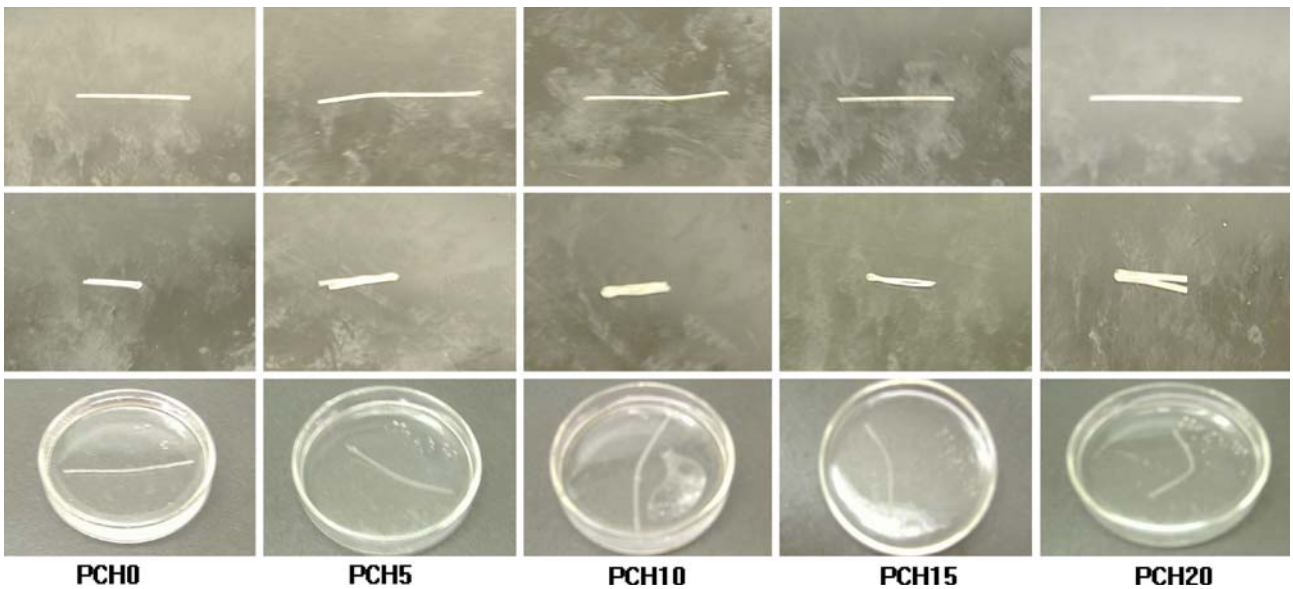

Fig. 8 The shape memory effect of the chitosan/PLLA (from *top* to *bottom*: permanent shape, deformed shape, and recovered shape)

Investigation of Shape Memory Properties

Shape Memory Behavior by Field Observation

Figure 8 shows the field observation results of the shape memory effect of chitosan/PLLA composites with different chitosan contents. The sample wires were prepared by using a Haake minilab extruder at 160 °C. Upon cooling to the ambient temperature, the wires' permanent straight shape was cast. If the samples were put into 65 °C hot water, they became very soft. At this temperature, the samples were folded in the middle and cooled to ambient temperature in air. As can be seen from Fig. 8, the deformed shapes are well fixed. After 2 min, the folded wires were put into 65 °C hot water to observe the shape recovery effect. As shown in Fig. 8, they recover their permanent straight shape quickly. However, with increasing chitosan contents, the deformed specimen cannot recover their permanent shapes completely. This suggests that the chitosan decreases the shape recovery degree of the PLLA.

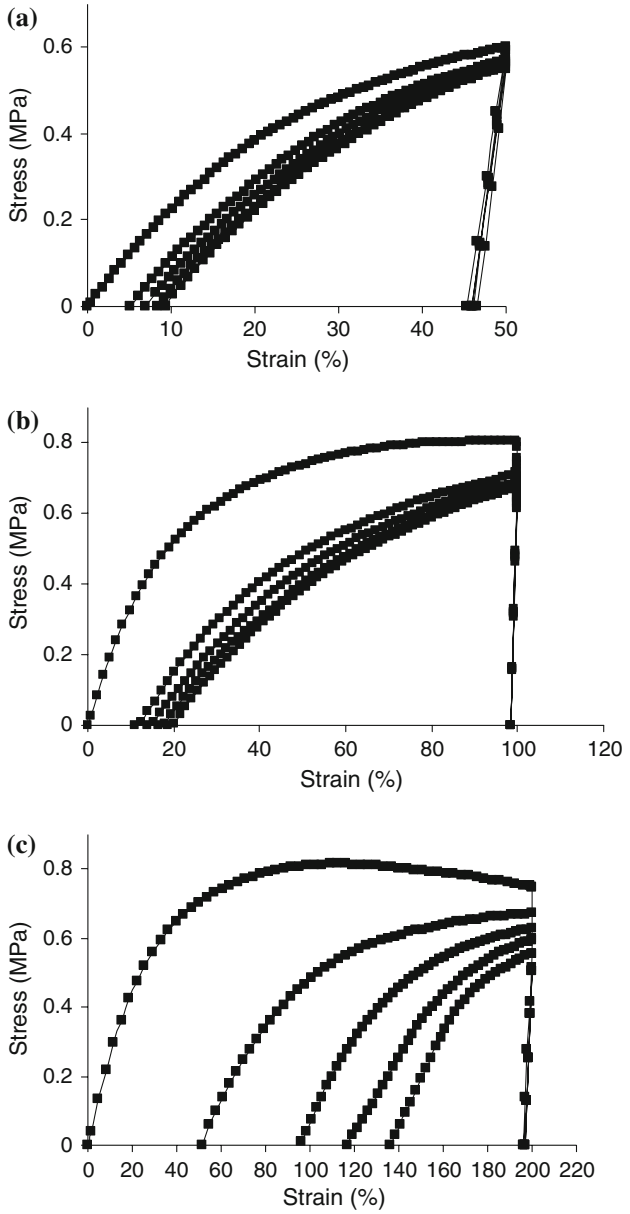

Fig. 9 The influence of deformation strain on the thermomechanical cyclic tensile curves of the PLLA. **a** 50%, **b** 100%, **c** 200%)

Thermomechanical Cyclic Tensile Tests

The Shape Memory Effect of PLLA To obtain the detailed shape memory properties of pure PLLA and chitosan/PLLA composites, thermomechanical cyclic tensile tests were conducted. The pre-set maximum strain ε_m in Fig. 3 was 50, 100 and 200%, respectively. The obtained cyclic tensile curves of pure PLLA are shown in Fig. 9, and the data of the fixity ratio, recovery ratio and stress at the maximum deformation strain are tabulated in Table 1.

In Fig. 9a and b, at 50 and 100% maximum deformation strain, good shape memory effect was observed. The significant difference between the first cycle and the remaining cycles is due to the reorganization of molecules involving molecule orientation, crystallization, or weak point broken during deformation. After one cycle, the stress–strain behaviors become very similar and stable.

Table 1 The shape memory properties of the PLLA at different deformation strain

Circle no.	εp(N) (%)	εu [R_f(N)] (%)	Stress at 100% max deformation strain (MPa)	Rr.tot(N) (%)
50% deformation strain				
1	0.0	90.8	0.588	100.00
2	10.4	91.8	0.554	89.60
3	14.0	91.8	0.545	86.00
4	16.0	92.1	0.532	84.00
5	18.7	92.8	0.582	81.30
100 deformation strain				
1	0.0	98.3	0.804	100.00
2	12.6	98.3	0.717	87.40
3	15.4	98.3	0.693	84.60
4	18.0	98.4	0.686	82.00
5	20.0	98.4	0.677	80.00
200 deformation strain				
1	0.0	98.0	0.750	100.00
2	25.5	98.3	0.670	74.50
3	48.0	98.5	0.630	52.00
4	58.5	98.6	0.595	41.50
5	68.0	98.7	0.555	32.00

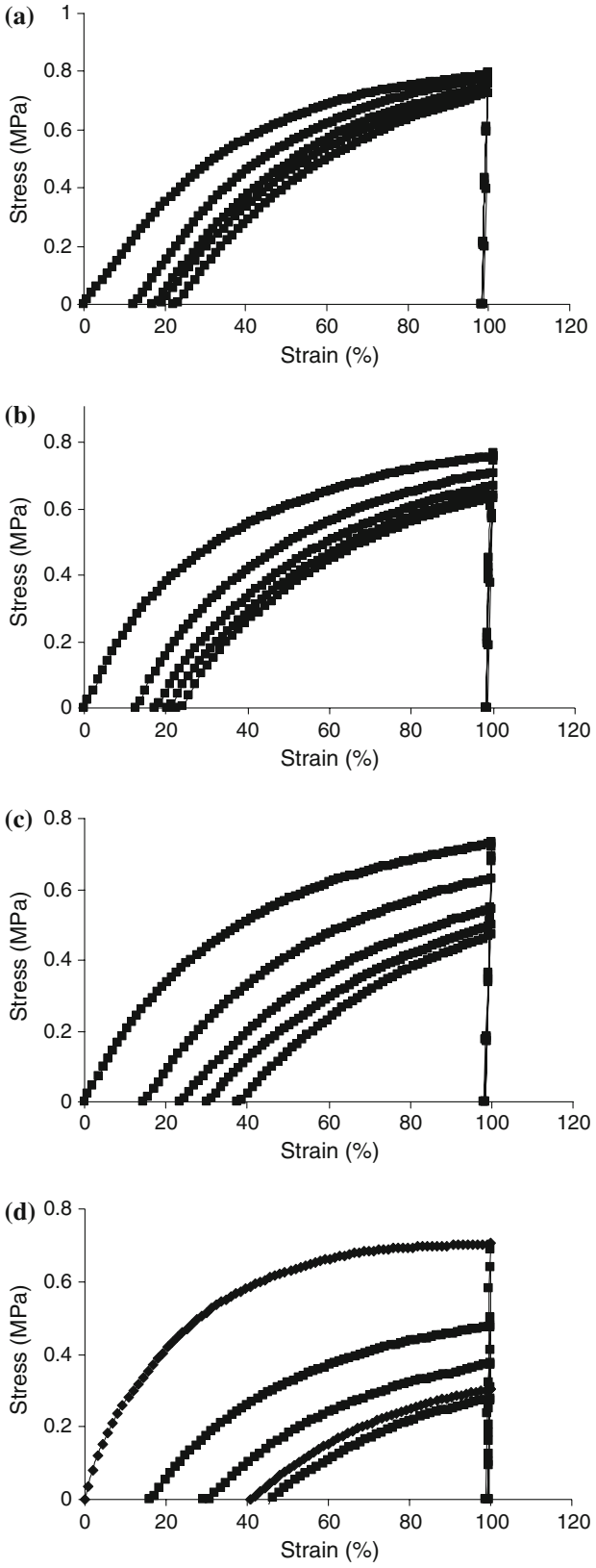

Fig. 10 The thermomechanical cyclic tensile testing curves of the chitosan/PLLA at different chitosan contents. **a** PCH5, **b** PCH10, **c** PCH15, **d** PCH20

However, in Fig. 9c, at 200% maximum deformation strain, the shape recovery ratios of the PLLA decrease significantly. In addition, the irrecoverable deformation increases severely with increasing testing cycles. This result indicates that the crystalline structure in PLLA which affords the shape recovery force may be substantially destroyed by the large deformation strain. As a result, PLLA, as a shape memory material, is not suitable for large deformation applications. Therefore, in the following studies of the shape memory effect of chitosan/PLLA composites, the maximum deformation strain was set as 100%.

The Influence of Chitosan on the Shape Memory Effect of PLLA The thermomechanical cyclic tensile curves of the chitosan/PLLA composites are shown in Fig. 10 and the corresponding shape fixity and recovery ratio are tabulated in Table 2. The chitosan has no obvious influence on the shape fixity ratio since the shape fixity ratios of pure PLLA and chitosan/PLLA composites are very high. However,

Table 2 The shape memory properties of chitosan/PLLA composites with different chitosan contents

Circle no.	εp(N) (%)	εu [Rf(N)] (%)	Stress at max deformation strain (MPa)	Rr.tot(N) (%)
PCH5				
1	0.0	98.2	0.789	100.00
2	12.6	98.4	0.777	87.40
3	17.8	98.4	0.751	82.20
4	20.4	98.4	0.736	79.60
5	23.0	98.6	0.723	77.00
PCH10				
1	0.0	98.2	0.755	100.00
2	13.2	98.2	0.708	86.80
3	18.0	98.3	0.673	82.00
4	21.2	98.3	0.641	78.80
5	24.0	98.6	0.633	76.00
PCH15				
1	0.0	98.3	0.730	100.00
2	14.5	98.3	0.628	85.50
3	23.5	98.3	0.546	76.50
4	30.2	98.4	0.499	69.80
5	37.6	98.4	0.471	62.40
PCH20				
1	0.0	98.9	0.704	100.00
2	16.8	99.2	0.477	83.20
3	30.5	99.3	0.374	69.50
4	41.0	99.4	0.305	59.00
5	46.2	99.5	0.276	53.80

chitosan decreases the shape recovery ratio markedly especially at high chitosan contents. As can be seen from Fig. 10d, the chitosan/PLLA composite at 20 wt% chitosan content has no significant shape memory effect after several cycles.

Table 3 The Elastic modulus ratio of glassy state to rubbery state of chitosan/PLLA composites

Sample	Glass transition T_g (°C)	Elastic modulus ratio[a]
PCH0	61.4	300
PCH5	60.2	175
PCH10	59.8	142
PCH15	60.2	105
PCH20	60.6	94

[a] Elastic modulus ratio was defined as $E'_{Tg-10\ °C}/E'_{Tg+10\ °C}$

One reason for the chitosan/PLLA having decreased shape memory effect is the decreased elastic modulus at the temperature below the switch temperature (glass transition temperature). It has been widely accepted that the good shape memory effect of polymers requires a rapid thermal transition from glassy state to rubbery state within a narrow temperature band, and a high elastic modulus ratio of glassy state modulus and rubbery state modulus. The higher the modulus ratio, the better the shape memory behavior of shape memory polymer would be [93–95]. The typical elastic modulus of shape memory polyurethanes is about 800 MPa in their glassy state and 2 MPa in their rubbery state [95–97], which means that the elastic modulus ratio of polyurethane is 400. In some special shape memory polyurethanes, the modulus ratio of the glassy state to the rubbery state may exceed 500. The elastic modulus ratios of the PLLA and its composites obtained by

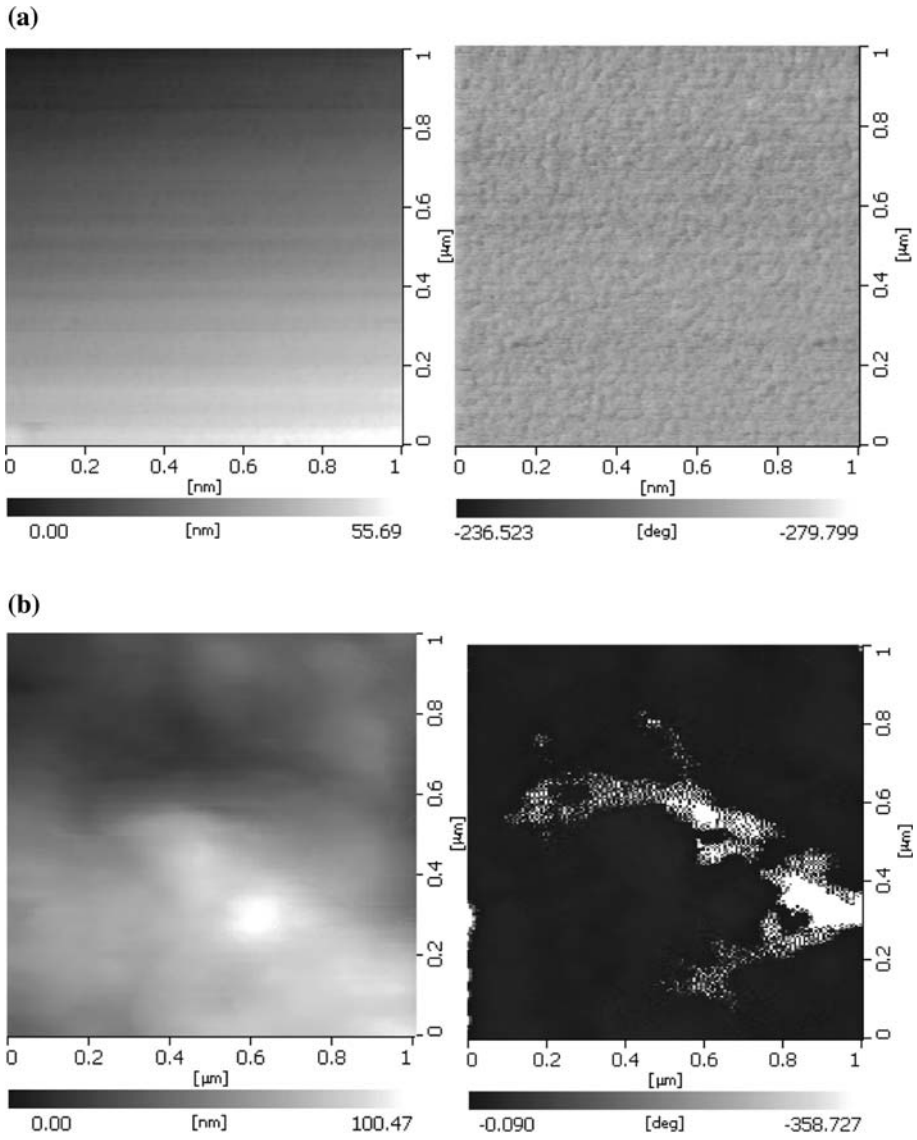

Fig. 11 The AFM images of the chitosan/PLLA at different chitosan contents (*left*: height image; *right*: phase image). **a** PCH0, **b** PCH5, **c** PCH10, **d** PCH15, **e** PCH20

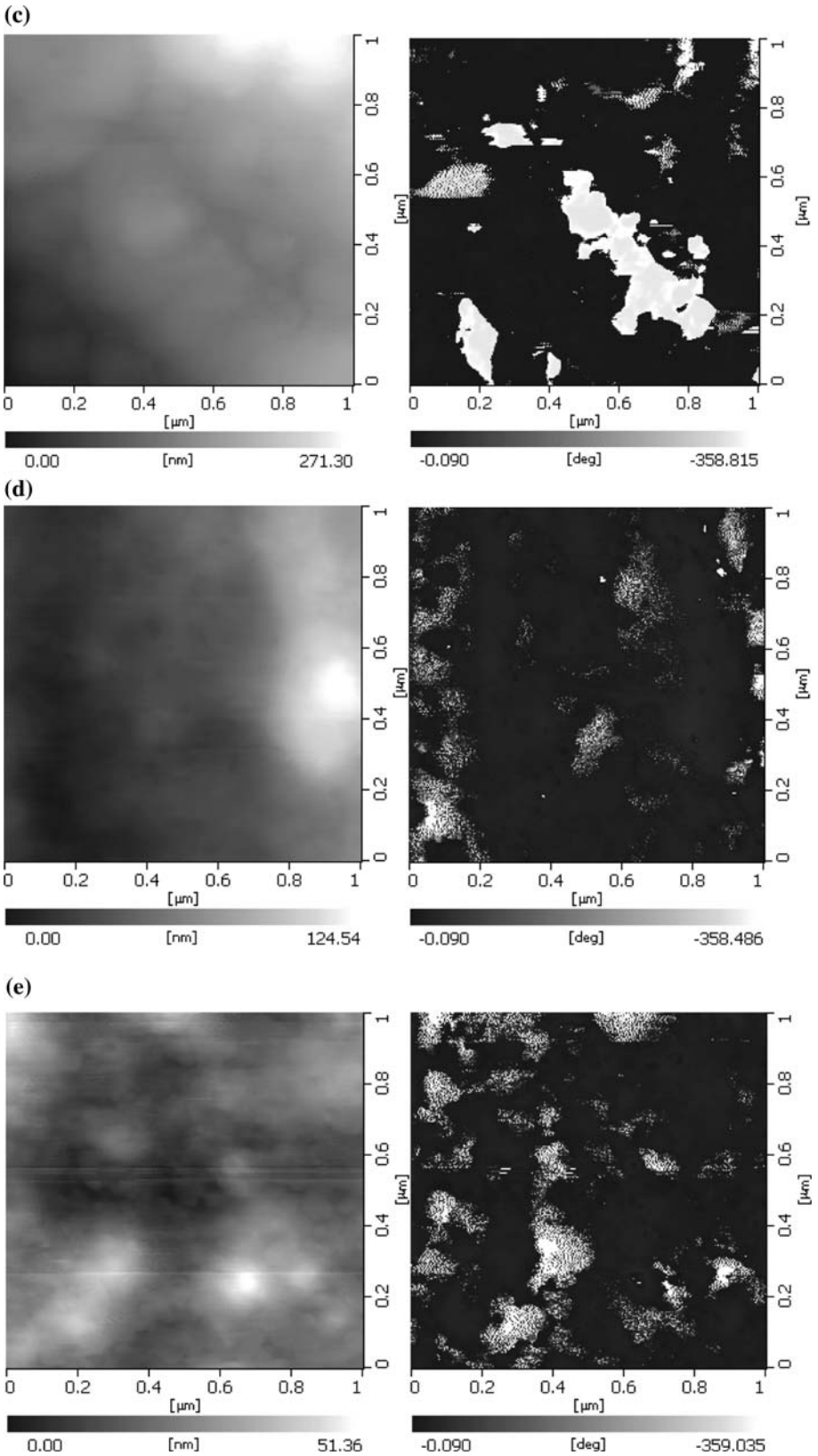

Fig. 11 continued

DMA are tabulated in Table 3. For the pure PLLA in this study, as can be seen from Table 3, the elastic modulus ratio is 300, which is lower than that of shape memory polyurethanes reported in the literature [98–100]. Therefore, the PLLA does not have so prominent shape memory effect as that observed on most shape memory polyurethanes. Table 3 also indicates that with increasing chitosan content, the elastic modulus ratio decreases greatly. Consequently, the shape recovery ratio of the PLLA decreases obviously with increasing chitosan contents.

Morphology Study

The AFM height and phase images of the pure PLLA and chitosan/PLLA composites are shown in Fig. 11. The phase images represent the variations of relative phase shifts (i.e. the phase angle of the interacting cantilever relative to the phase angle of the freely oscillating cantilever at the resonance frequency) and are thus able to distinguish phases by the materials properties.

As can be seen in Fig. 11, no phase separation structure is observed on the pure homopolymer PLLA as those in segmented polyurethane copolymers with phase separation structures [101–104]. According to the mechanism of the shape memory effect for segmented copolymers, the formation of a stable hard segment phase and high degree of phase separation between the hard segment phase and the reversible soft segment phase is necessary for shape memory polymers to show good shape memory effects [80, 105–107]. The shape memory effect of PLLA is because of the viscoelastic properties of PLLA comprising crystalline and glassy structures. The crystalline structure having a higher melting temperature is responsible for internal stress storing and releasing during the shape deformation and recovery process, while the glassy structure with a lower glass transition acting as a switch is in charge of shape fixity.

In AMF phase images in Fig. 11, obvious phase separation structures are observed in the chitosan/PLLA composites. The above results demonstrate that the phase separation does not contribute to the good shape memory effect of the PLLA. On the contrary, the phase separation deteriorates the shape memory effect of the PLLA. With increasing chitosan contents, the shape recovery ratio of the composites decreases obviously.

The DMA has demonstrated that the modulus of the chitosan/PLLA composites decreases with increasing chitosan content. The lack of miscibility between PLLA and chitosan may lead to the formation of pores [108, 109] due to the debonding of the chitosan and PLLA matrix upon the application of deformation during the cyclic tensile testing. In the cyclic shape memory process, when the composites is deformed and cooled to a temperature below the glass transition temperature, due to the formation of pores because of the immiscibility of PLLA and chitosan, the internal stress cannot be stored efficiently in the composites. If the composites are reheated to above the glass transition temperature, the glassy state phase undergoes phase transition from a glassy state to a rubbery state. The composites modulus decrease and consequently the stored internal stress in the composites release. Because the composites, especially at high chitosan content, cannot effectively store internal stress, the shape recovery ratio decreases significantly.

Conclusions

The shape memory effect of chitosan/PLLA composites was studied. The shape memory effect of the composites arises from the viscoelastic properties of the PLLA composed of the amorphous structure and crystalline structure. PLLA as a shape memory polymer cannot be subject to large deformation strains. The maximum deformation strain should be below 200%. PLLA and chitosan were compounded to make novel materials which may have biodegradability and biocompatibility. Chitosan does not significantly affect the glass and melting transition temperature of the PLLA. Phase separation structures of the composites were observed. The shape recovery ratio of the polymer decreases dramatically with increasing chitosan contents due to the immiscibility between chitosan and PLLA. To obtain good shape memory effect of the composites, the chitosan content should be below 15 wt%.

References

1. Gutowska A, Bae YH, Jacobs H, Feijen J, Kim SW (1994) Thermosensitive interpenetrating polymer network: synthesis, characterisation, and macromolecular release. Macromolecules 27:4167–4175
2. Asaka K, Oguro K (2000) Bending of polyelectrolyte membrane platinum composites by electric stimuli. J Electroanal Chem 480:186–198
3. Feil H, Bae YH, Feijen T, Kim SW (1992) Mutual influence of pH and temperature on the swelling of ionizable and thermosensitive hydrogels. Macromolecules 25:5228–5230
4. Siegal RA, Firestone BA (1988) pH-dependent equilibrium swelling properties of hydrophobic polyelectrolyte copolymer gels. Macromolecules 21:3254–3259
5. Jiang HY, Kelch S, Lendlein A (2006) Polymers move in response to light. Adv Mater 18:1471–1475
6. Makhosaxana XP, Filipcsei G, Zrınyi M (2000) Preparation and responsive properties of magnetically soft poly(*N*-isopropylacrylamide) gels. Macromolecules 33:1716–1719
7. Hu JL, Meng QH, Zhu Y, Lu J, Zhuo HT (2007) Shape memory fibers prepared by wet, reaction, dry, melt, and electro spinning. US Patent 11/907,012, 6 Oct 2007

8. Meng QH, Hu JL, Zhu Y, Lu J, Liu Y (2007) Morphology, phase separation, thermal and mechanical property differences of shape memory fibres prepared by different spinning methods. Smart Mater Struct 16:1192–1197
9. Lendlein A, Langer R (2002) Biodegradable, elastic shape-memory polymers for potential biomedical applications. Science 96:1673–1676
10. Metcalfe A, Desfaits A-C, Salazkin I, Yahiab L, Sokolowskic WM, Raymonda J (2003) Cold hibernated elastic memory foams for endovascular interventions. Biomaterials 24:491–497
11. Wache HM, Tartakowska DJ, Hentrich A, Wagner MH (2004) Development of a polymer stent with shape memory effect as a drug delivery system. J Mater Sci Mater Med 14:109–112
12. Langer R, Tirrell DA (2004) Designing materials for biology and medicine. Nature 428:487–492
13. Laroche FEFG, Fiset M, Mantovani D (2002) Shape memory materials for biomedical applications. Adv Eng Mater 4:91–104
14. Sharp AA, Panchawagh HV, Ortega A, Artale R, Richardson-Burns S, Finch DS, Gall K, Mahajan RL, Restrepo D (2006) Toward a self-deploying shape memory polymer neuronal electrode. J Neural Eng 3:L23–L30
15. Charlesby A (1960) Atomic radiation and polymers. Pergamon Press, New York, pp 198–257
16. Hu JL, Ding XM, Tao XM (2002) Shape memory polymers and their applications to smart textile products. J China Textile Univ 19:89–93
17. Fan HJ, Hu JL, Ji FL (2004) Environmental-benign thermal-sensitive polyurethane for textile finishing. Paper presented at the world textile conference 4th AUTEX conference, Roubaix, France, June 22–24, 2004
18. Russel DA, Hayashi S, Yamada T (1999) The potential use of memory film in clothing. Paper presented at the Techtextil symposium-new protective textiles (through textile technology index database)
19. Russel A, Hayashi S, Yamada T (1999) Potential use of shape memory film in clothing. Tech Text Int 8:17–19
20. Ji FL, Zhu Y, Hu JL, Liu Y, Yeung LY, Ye GD (2006) Smart polymer fibers with shape memory effect. Smart Mater Struct 15:1547–1554
21. Zhu Y, Jl Hu, Yeung LY, Liu Y, Ji FL, Yeung KW (2006) Development of shape memory polyurethane fiber with complete shape recoverability. Smart Mater Struct 15:1385–1394
22. Meng QH, Hu JL (2007) Study on poly(ε-caprolactone)-based shape memory copolymer fiber prepared by bulk polymerization and melt spinning. Polym Adv Technol. doi:10.1002/pat.985
23. Meng QH, Hu JL, Zhu Y, Lu J, Liu Y (2007) Polycaprolactone-based shape memory segmented polyurethane fiber. J Appl Polym Sci 106:2515–2523
24. Hu JL, Meng QH, Zhu Y, Lu J, Zhuo HT (2007) Shape memory fibers prepared by wet, reaction, dry, melt, and electro spinning. US Patent 11/907,012 in USA, 9 Oct 2007
25. Jeong HM, Ahn BK, Cho SM, Kim BK (2000) Water vapor permeability of shape memory polyurethane with amorphous reversible phase. J Polym Sci B Polym Phys 38:3009–3017
26. Jeong HM, Ahn BK, Kim BK (2000) Temperature sensitive water vapour permeability and shape memory effect of polyurethane with crystalline reversible phase and hydrophilic segments. Polym Int 49:1714–1721
27. Chen W, Zhu CY, Gu XR (2002) Thermosetting polyurethanes with water-swollen and shape memory properties. J Appl Polym Sci 84:1504–1512
28. Mondal S, Hu JL (2006) Structural characterization and mass transfer properties of nonporous segmented polyurethane membrane: influence of hydrophilic and carboxylic group. J Membr Sci 274:219–226
29. Mondal S, Hu JL (2006) Structural characterization and mass transfer properties of nonporous-segmented polyurethane membrane: influence of the hydrophilic segment content and soft segment melting temperature. J Membr Sci 276:16–22
30. Mondal S, Hu JL (2007) A novel approach to excellent UV protecting cotton fabric with functionalized MWNT containing water vapor permeable PU coating. J Appl Polym Sci 103:3370–3376
31. Mondal S, Hu JL (2007) Water vapor permeability of cotton fabrics coated with shape memory polyurethane. Carbohydr Polym 67:282–287
32. Mondal S, Hu JL, Zhu Y (2006) Free volume and water vapor permeability of dense segmented polyurethane membrane. J Membr Sci 280:427–432
33. Chen H, Hsieh Y-L (2004) Ultrafine hydrogel fibers with dual temperature- and pH-responsive swelling behaviors. J Polym Sci A Polym Chem 42:6331–6339
34. Chen H, Palmese GR, Elabd YA (2005) Polyester-poly(methacrylic acid) nanocomposite membranes as breathable barriers. ACS Polym Preprint 46:1202–1203
35. Tobushi H, Hayashi S, Hoshio K, Miwa N (2006) Influence of strain-holding conditions on shape recovery and secondary-shape forming in polyurethane-shape memory polymer. Smart Mater Struct 15:1033–1038
36. Tobushi H, Matsui R, Hayashi S, Shimada D (2004) The influence of shape-holding conditions on shape recovery of polyurethane-shape memory polymer foams. Smart Mater Struct 13:881–887
37. Marco D, Eckhouse S (2006) Biodegradable self-inflating intragastric implants for curbing appetite. US Patent 20070156248 in USA
38. Lendlein A, Langer RS (2004) Self-expanding device for the gastrointestinal or urogenital area. WO/2004/073690, PCT/US2004/004776 in USA
39. Hayashi S, Tasaka Y, Hayashi N, Akita Y (Feb 2004) Development of smart polymer materials and its various applications. Technical review, vol 41, No 1. Mitsubishi Heavy Industries, Ltd
40. Liu C, Qin H, Mather PT (2007) Review of progress in shape-memory polymers. J Mater Chem 17:1543–1558
41. Maitland DJ, Metzger MF, Schumann D, Lee A, Wilson TS (2002) Photothermal properties of shape memory polymer micro-actuators for treating stroke. Lasers Surg Med 30:1–11
42. Small W IV, Wilson TS, Benett WJ, Loge JM, Maitland DJ (2005) Laser-activated shape memory polymer intravascular thrombectomy device. Opt Express 13:8204–8213
43. Small W IV, Metzger MF, Wilson TS, Maitland DJ (2005) Laser-activated shape memory polymer microactuator for thrombus removal following ischemic stroke: preliminary in vitro analysis. IEEE J Sel Top Quantum Electron 11:892–901
44. Buckley PR, McKinley GH, Wilson TS, Small W IV, Benett WJ Bearinger JP, McElfresh MW, Maitland DJ (2006). Inductively heated shape memory polymer for the magnetic actuation of medical devices. Paper presented at the IEEE transactions on biomedical engineering
45. Schmidt AM (2006) Electromagnetic activation of shape memory polymer networks containing magnetic nanoparticles. Macromol Rapid Commun 27:1168–1172
46. Hampikian JM, Heaton BC, Tong FC, Zhang Z, Wong CP (2006) Mechanical and radiographic properties of a shape memory polymer composite for intracranial aneurysm coils. Mater Sci Eng C 26:1373–1379
47. Smart Surgery (2004) Future materials (through textile technology index), pp 33–34
48. Langer RS, Lendlein A (2003) biodegradable shape memory polymeric sutures. World Patent WO 2003088818 A2

49. Huang WM, Lee CW, Teo HP (2006) Thermomechanical behavior of a polyurethane shape memory polymer foam. J Intell Mater Syst Struct 17:753–760
50. Yasuo S (1998) Shape-memory, biodegradable and absorbable material. US Patent19980189973
51. Mather PT, Liu C, Burstone CJ (Dec, 2005) Shape memory polymer orthodontic appliances, and methods of making and using the same. European Patent EP1844097, World Patent 2006071520, 2006
52. Liu C, Mather PT, Burstone C (2006) Proceedings of the annual technical conference—society of plastics engineers, 64th, society of plastics engineers, Brookfield, CT, USA, pp 1356–1360
53. Ikada Y, Tsuji H (2000) Biodegradable polyesters for medical and ecological applications. Macromol Rapid Commun 21:117–132
54. Urayama H, Kanamori T, Kimura Y (2002) Properties and biodegradability of polymer blends of poly(L-lactide)s with different optical purity of the lactate units. Macromol Mater Eng 287:116–121
55. Penning JP, Grijpma DW, Pennings AJ (1993) Hot-drawing of poly(lactide) networks. J Mater Sci Lett 12:1048–1051
56. Schakenraad JM, Hardonk MJ, Feijen J, Molenaar I (1990) Enzymatic activity toward poly (L-lactic acid) implants. J Biomed Mater Res 24:529–545
57. Schakenraad JM, Oosterbaan JA, Nieuwenhuis P (1988) Biodegradable hollow fibres for the controlled release of drugs. Biomaterials 9:116–120
58. Kim HD, Bae EH, Kwon IC, Pal RR, Nam JD, Lee DS (2004) Effect of PEG-PLLA diblock copolymer on macroporous PLLA scaffolds by thermally induced phase separation. Biomaterials 25:2319–2329
59. Yoshimoto H, Shin YM, Terai H, Vacanti JP (2003) A biodegradable nanofiber scaffold by electrospinning an its potential for bone tissue engineering. Biomaterials 24:2077–2082
60. Leenslag JW, Pennings AJ, Bos R, Rozema FR, Boering G (1987) Resorbable materials of poly(L-lactide). VI. In vivo and in vitro degradation. Biomaterials 8:311–314
61. Bos RRM, Rozema FR, Boering G (1991) Degradation of and tissue reaction to biodegradable poly(L-lactide) for use as internal fixation of fractures. A study in rats. Biomaterials 12:32–36
62. Lu X, Sun Z, Cai W (2007) Structure and shape memory effects of poly(L-lactide) and its copolymers. Physica Scripta T:T129. Second international symposium on functional materials, 2007, pp 231–235
63. Lu X, Cai W, Zhao L (2005) Study on the shape memory behavior of poly(L-lactide). Mater Sci Forum 475–479(III). PRICM 5: the fifth pacific rim international conference on advanced materials and processing, 2005, pp 2399–2402
64. Shikinami Y (2001) Shape memory biodegradable and absorbable material. US Patent 6281262 B1
65. Jordan G (2008) Balloon Geometry for delivery and deployment of shape memory polymer stent with flares. US Patent 20080132988
66. Moaddeb S, Shaolian SM, Shaoulian E, Rhee R, Anderson SC (2007) Shape memory devices and methods for reshaping heart anatomy. US Patent 7285087
67. Mather PT, Liu C, Campo CJ (2007) blends of amorphous and semicrystalline polymers having shape memory properties. US Patent 7208550
68. Zheng X, Zhou S, Li X, Weng J (2006) Shape memory properties of poly(D, L-lactide)/hydroxyapatite composites. Biomaterials 27:4288–4295
69. Knowles J, Roller S (2001) Efficacy of chitosan, carvacrol, and a hydrogen peroxide-based biocide against foodborne microorganisms in suspension and adhered to stainless steel. J Food Protect 64:1542–1548
70. Helander IM N-LE, Ahvenainen R, Rhoades J, Roller S (2001) Chitosan disrupts the barrier properties of the outer membrane of gram-negative bacteria. Int J Food Microbiol 71:235–244
71. Liu HYD, Wang X, Sun L (2004) Chitosan kills bacteria through cell membrane damage. Int J Food Microbiol 95:147–155
72. Je J, Kim S (2006) Antimicrobial action of novel chitin derivative. Biochim Biophys Acta 1760:104–109
73. Zhu A, Zhang M, Wu J, Shen J (2002) Covalent immobilization of chitosan/heparin complex with a photosensitive heterobifunctional crosslinking reagent on PLA surface. Biomaterials 23:4657–4665
74. Li L, Ding S, Zhou C (2004) Preparation and degradation of PLA/chitosan composite materials. J Appl Polym Sci 91:274–277
75. Sébastien F, Stéphane G, Copinet A, Coma V (2006) Novel biodegradable films made from chitosan and poly(lactic acid) with antifungal properties against mycotoxinogen strains. Carbohydr Polym 65:185–193
76. Suyatma NE, Copinet A, Tighzert L, Coma V (2004) Mechanical and barrier properties of biodegradable films made from chitosan and poly (lactic acid) blends. J Polym Environ 12(1):1–6
77. Merck D (1988) Merck FT-IR Atlas. VCH Publishers
78. Hu JL, Ji FL, Wong YW (2005) Dependency of the shape memory properties of a polyurethane upon thermomechanical cyclic conditions. Polym Int 54:600–605
79. Lendlein A, Kelch S (2002) Shape-memory polymers. Angew Chem Int Ed 41:2034–2057
80. Kim BK, Lee SY, Xu M (1996) Polyurethane having shape memory effect. Polymer 37:5781–5793
81. Meng QH, Hu JL, Zhu Y (2007) Shape-memory polyurethane/multiwalled carbon nanotube fibers. J Appl Polym Sci 106:837–848
82. Ray S, Yamada K, Okamoto M, Ogami A, Ueda K (2003) New polylactide/layered silicate nanocomposites. 3. High-performance biodegradable materials. Chem Mater 15:1456–1465
83. Ray S, Yamada K, Okamoto M, Fujimoto Y, Ogami A, Ueda K (2003) New polylactide/layered silicate nanocomposites. 5. Designing of materials with desired properties. Polymer 44:6633–6646
84. Marras SI, Zuburtikudis I, Panayiotou C (2007) Nanostructure versus microstructure: morphological and thermomechanical characterization of poly(L-lactic acid)/layered silicate hybrids. Eur Polym J 43:2191–2206
85. Xiao Hu H-SX, Zhong-Ming Li (2007) Morphology and properties of poly(L-lactide) (PLLA) filled with hollow glass beads. Macromol Mater Eng 292:646–654
86. Correlo VM, Boesel LF, Bhattacharya M, Mano JF, Neves NM, Reis RL (2005) Properties of melt processed chitosan and aliphatic polyester blends. Mater Sci Eng A 403:57–68
87. Lewitus D, McCarthy S, Ophir EA, Kenig S (2006) The effect of nanoclays on the properties of PLLA-modified polymers part 1: mechanical and thermal properties. J Environ Polym Degr 14:171–177
88. Miyata T, Masuko T (1998) Crystallization behaviour of poly(L-lactide). Polymer 39:5515–5521
89. Srimoaon P, Dangseeyun N, Supaphol P (2004) Multiple melting behavior in isothermally crystallized poly(trimethylene terephthalate). Eur Polym J 40:599–608
90. Supapho P (2001) Crystallization and melting behavior in syndiotactic polypropylene: origin of multiple melting phenomenon. J Appl Polym Sci 82:1083–1097
91. Ke T, Sun X (2003) Melting behavior and crystallization kinetics of starch and poly(lactic acid) composites. J Appl Polym Sci 89:1203–1210
92. Meng QH, Hu JL (2008) Self-organizing alignment of carbon nanotube in shape memory segmented fiber prepared by in situ polymerization and melt spinning. Compos A 39:314–321

93. Lin JR, Chen LW (1998) Study on shape-memory behavior of polyether-based polyurethanes. II. Influence of soft-segment molecular weight. J Appl Polym Sci 69:1575–1586
94. Cao Y, Guan Y, Du J, Luo J, Peng Y, Yip CW, Chan ASC (2002) Hydrogen-bonded polymer network-poly(ethylene glycol) complexes with shape memory effect. J Mater Chem 12:2957–2960
95. Wei ZG, Sandstrom R, Miyazaki S (1998) Shape-memory materials and hybrid composites for smart systems: part I shape-memory materials. J Mater Sci 33:3743–3762
96. Meng Q, Hu J, Zhu Y (2008) Properties of shape memory polyurethane used as a low temperature thermoplastic orthotic material: influence of hard segment content. J Biomater Sci Polym Edn 19:1437–1454
97. Meng QH, Hu JL, Mondal S (2008) Thermal sensitive shape recovery and mass transfer properties of polyurethane/modified MWNT composite membranes synthesized via in situ solution pre-polymerization. J Membr Sci 319:102–110
98. Lee BS, Chun BC, Chung Y-C, Sul KI, Cho JW (2001) Structure and thermomechanical properties of polyurethane block copolymers with shape memory effect. Macromolecules 34:6431–6437
99. Li FK, Zhang X, Hou JA, Xu M, Luo XL, Ma DZ, Kim BK (1996) Studies on thermally stimulated shape memory effect of segmented polyurethanes. J Appl Polym Sci 64:1511–1516
100. Kim BK, Lee SY (1998) Polyurethane ionomers having shape memory effects. Polymer 39:2803–2808
101. Garrett JT, Siedlecki CA, Runt J (2001) Microdomain morphology of poly(urethane urea) multiblock copolymers. Macromolecules 34:7066–7070
102. Tan H, Li J, Guo M, Du R, Xie X, Zhong Y, Fu Q (2005) Phase behavior and hydrogen bonding in biomembrane mimicing polyurethanes with long side chain fluorinated alkyl phosphatidylcholine polar head groups attached to hard block. Polymer 46:7230–7239
103. McLean RS, Sauer BB (1997) Tapping-mode AFM studies using phase detection for resolution of nanophases in segmented polyurethanes and other block copolymers. Macromolecules 30:8314–8317
104. Aneja A, Wilkes GL (2004) Hard segment connectivity in low molecular weight model 'trisegment' polyurethanes based on monols. Polym 45:927–935
105. Li SY, Tang XZ, Luo YP, Xu XM (1998) The study of a thermoplastic polyurethane ionomer system. Eur Polym J 34:1899–1902
106. Tobushi H, Hashimoto T, Ito N, Hayashi S, Yamada E (1998) Shape fixity and shape recovery in a film of shape memory polymer of polyurethane series. J Intell Mater Syst Struct 9:127–136
107. Bogdanov B, Toncheva V, Schacht E, Finelli L, Sarti B, Scandol M (1999) Physical properties of poly(ester-urethanes) prepared from different molar mass polycaprolactone-diols. Polymer 40:3171–3182
108. Peesan M, Supaphol P, Rujiravanit R (2005) Preparation and characterization of hexanoyl chitosan/polylactide blend films. Carbohydr Polym 60:343–350
109. Peesan M, Supaphol P, Rujiravanit R (2007) Effect of casting solvent on characteristics of hexanoyl chitosan/polylactide blend films. J Appl Polym Sci 105:1844–1852